



Research article

Study on Mudcake disintegration in clayey strata during shield tunneling: Effects of dispersants and bentonite slurry

Pengfei Liu^{a,b,c,*}, Zhao Yang^a, Fuquan Ji^a, Peishuai Chen^a, Qinxin Hu^d, Xiong He^a^a CCCC Second Harbor Engineering Company Ltd., Wuhan, Hubei, 430012, China^b Key Laboratory of Safe Construction and Intelligent Maintenance for Urban Shield Tunnels of Zhejiang Province, Hangzhou, Zhejiang, 310015, China^c Institute of Rock and Soil Mechanics, Chinese Academy of Sciences, Wuhan, Hubei, 430071, China^d Department of Civil and Environmental Engineering, University of Strathclyde, Glasgow, G1 1XJ, UK

ARTICLE INFO

Keywords:

Shield tunnel
Clayey strata
Shield clogging
Mudcake disintegration
Dispersant

ABSTRACT

While tunnel boring machines (TBMs) tunneling in clayey strata, the adhered excavated soil on the cutterhead and cutting tools tends to form mudcake after compaction and consolidation. Mudcake can obstruct the cutterhead openings and rendering the cutting tools ineffective, leads to a substantial reduction in advance rate. Dispersants are recognized as an effective method for the disintegration of mudcakes. A novel set of equipment, comprising a mudcake compression device and a mudcake disintegration apparatus, is developed for assessing mudcake disintegration properties. The results showed that mudcakes underwent a tripartite disintegration process in water, including an initial stage, a rapid disintegration stage, and a stable stage. In the initial stage, the mudcakes absorbed water before disintegration, resulting in marginal changes in the weight of the disintegrated mudcakes. In the rapid disintegration stage, the weight of the disintegrated mudcakes increased quickly. During the stable stage, the weight of the disintegrated mudcakes remained relatively constant. The submersion of mudcakes in a dispersant solution substantially increased the rate of disintegration. Greater dispersant concentration corresponded to an increase in the disintegration rate. No weight gain was observed in mudcakes during the initial disintegration stage. When mudcakes disintegrated in a bentonite slurry, the weight of the disintegrated mudcakes initially decreased and then stabilized. The weight of the disintegrated mudcakes turned negative, indicating an increase in the weight of mudcakes. This suggested that bentonite significantly hindered mudcake disintegration.

1. Introduction

Compared to traditional mining methods, the shield tunneling method has several advantages, such as higher safety [1] and lower construction cost [2] and adverse environmental impact [3]. Thus, it is commonly used in tunnel construction [4]. The commonly used shield tunneling methods include earth pressure balance (EPB) shield tunneling and slurry pressure balance (SPB) shield tunneling [5]. Regardless of whether it is an EPB shield tunneling or a SPB shield tunneling, excavated soil adheres to the cutterhead and cutting tools during shield tunneling through clayey strata [6]. Due to the force applied by the shield tunnel, the soil particles adhering to the cutterhead and tools amalgamate, forming mudcakes [7]. Mudcake is a semi-consolidated or consolidated mass formed by the fine

* Corresponding author. CCCC Second Harbor Engineering Company Ltd., Wuhan, Hubei, 430040, China.
E-mail address: pfliu0229@foxmail.com (P. Liu).

<https://doi.org/10.1016/j.heliyon.2024.e30663>

Received 11 December 2023; Received in revised form 12 April 2024; Accepted 1 May 2024

Available online 3 May 2024

2405-8440/© 2024 The Authors. Published by Elsevier Ltd. This is an open access article under the CC BY-NC-ND license (<http://creativecommons.org/licenses/by-nc-nd/4.0/>).

particles, which re-aggregate in the shield chamber and cutterhead area. Therefore, it has high strength, with some mudcakes exhibiting compressive strengths exceeding 5 MPa. Mudcake formation affects the shield tunneling process, such as higher thrust demands [8], lower advancement rates [9], and increased tool wear [10]. These changes together decrease the overall efficiency of construction.

Many researchers around the world have investigated ways to prevent mudcake formation during shield tunneling [11]. In the context of EPB shield tunneling, the state of the excavated soil strongly influences the development of mudcakes [12]. Applying soil conditioning techniques to alter the soil state can effectively reduce the adhesion of soil to the shield machine [13], thus preventing mudcake formation [14,15]. Wang et al. [16] used interfacial adhesion forces to assess the adhesive properties of soil samples and found that the critical particle size for mudcake formation in shield tunneling is 0.15 mm. According to Maidl et al. [17], when the consistency index is around 0.40–0.75, soil has difficulty adhering to the shield cutterhead or cutter tools. Under this condition, the soil can efficiently transmit earth pressure and prevent mudcake formation. By conducting mixing tests, Zumsteg and Puzrin [18,19] found that the inclusion of dispersants considerably decreased soil adhesion when the plasticity index was below 0.8. Oliveira et al. [20,21] used a similar mixing apparatus to assess the adhesive traits of cohesive soil. They found that the optimal plasticity index for cohesive soil was within 0.4–0.5. These findings were similar to those of Hollmann and Thewes [22], who conducted field experiments. Liu et al. [23] and Wang et al. [24] recommended that maintaining a consistency index below 0.5 can avoid mudcake formation in shield tunneling. In the context of slurry balance shield tunneling, mudcake formation is prevented primarily via cutterhead flushing. Xiao et al. [25] used Computational Fluid Dynamics (CFD) to simulate the flushing process in the central pipe of the cutterhead. They showed that the convergence angle and aspect ratio are key parameters that influence the flushing performance. Liu et al. [26] proposed the application of an anti-adhesive coating on the surface of the shield cutterhead and cutting tools to reduce soil adhesion and prevent mudcake formation. However, their approach had low efficacy due to the susceptibility of the coating to wear during the tunneling process.

When mudcakes accumulate on the cutterhead of a shield tunnel, the excavation speed decreases significantly. Common methods for removing mudcakes include high-pressure cutting, dispersant removal, and manual cleaning [27]. High-pressure cutting requires the shield machine to be equipped with specialized equipment, which can be costly. Manual cleaning poses a greater safety risk to construction workers. Dispersant removal is the safest and most cost-effective method for treating mudcakes [28]. The application of chemical agents disintegrates mudcakes via a process analogous to soil slaking. The process of soil slaking undergoes a series of physical and oxidative reactions [29]. Many researchers have investigated soil slaking mechanisms. Bissonnais [30] and Emerson [31] suggested that the extent of soil microstructure dispersion is associated with the total electrolyte concentration (TEC) in the solution and the exchangeable sodium percentage (ESP) in the soil. Lower total electrolyte concentrations and higher exchangeable sodium percentages result in greater clay dispersion. Shainberg and Letey [32] showed a relationship between soil dispersion and total electrolyte concentration. When the electrolyte concentration of the solution increases, the double-layer thickness is compressed, leading to a reduction in the overlap of the two layers between soil particles and a decrease in the repulsive forces among particles. These changes are detrimental to soil dispersion. Quirk [33] found that when the ion concentration at the midplane between particles exceeds the external ion concentration within the pores of clay aggregates, the concentration differential generates an osmotic pressure

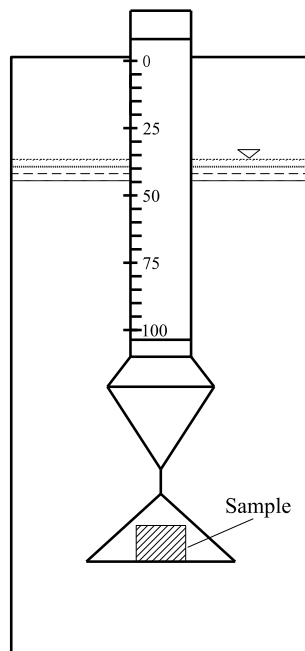


Fig. 1. Traditional disintegration apparatus.

gradient. This phenomenon draws water between the particles, causing particle movement or clay swelling, resulting in the disintegration of soil aggregates.

Mudcake formation still occurs during shield tunneling in cohesive soil strata due to construction constraints, even after implementing the measures to prevent mudcake formation suggested by researchers. Once mudcakes form on the shield, they need to be immersed in dispersants to be disintegrated. However, there are many types of dispersants currently, necessitating a reliable method for evaluating the effectiveness of dispersants. The traditional buoyancy-based disintegration apparatus relies on the Archimedes principle (Fig. 1). The float is prone to vertical movement during the reading process, leading to poor accuracy of the instrument. In addition, it is difficult to accurately read through the cylinder wall. Fang et al. [27] made improvements on the traditional buoyancy-based disintegration apparatus by using an electronic tension meter instead of a float, enhancing the accuracy of test data (Fig. 2). However, suspending the sample with flexible ropes led to poor instrument stability, resulting in high reading fluctuations. Additionally, the authors did not develop a dedicated mudcake compression device. Thus, there still is a lack of suitable instruments and methodologies to evaluate the characteristics of mudcake disintegration under the influence of dispersants, although several studies have focused on soil disintegration and its mechanisms. In addition, the mudcake in slurry shield tunneling is immersed in the slurry after formation. The slurry in slurry balance shield tunneling can affect the efficiency of mudcake disintegration. Several researchers in the drilling industry have pointed out that the presence of slurry can form a mudskin on the soil surface, inhibiting soil disintegration [34]. However, information on the influence of slurry on mudcake disintegration characteristics is limited.

In order to investigate the disintegration characteristics of mudcakes, this study first developed a mudcake compression device capable of pressing mudcake samples with different degrees of saturation and water content. Subsequently, a more stable mudcake disintegration apparatus was developed. Using the mudcake compression device, mudcakes of the same compactness as those on construction sites were pressed. The disintegration curve of the pressed mudcakes was obtained using the mudcake disintegration apparatus, which were used for a comprehensive analysis of the patterns of mudcake disintegration. The effect of dispersants on mudcake disintegration was further explored. Finally, the disintegration characteristics of mudcakes in slurry were analyzed.

2. Testing materials and approach

2.1. Background

The total length of the shield tunneling section is 1332.9 m in Metro Line 12 in Guangzhou. The tunnel is primarily found in formations of fully weathered silty sandstone, highly weathered silty sandstone, and moderately weathered silty sandstone [35]. Table 1 shows the physical and mechanical parameters of each layer. The fully weathered silty sandstone formation has silt and clay contents of 42 % and 23 % respectively, and it exhibits a cohesive strength of 30 kPa. The highly weathered silty sandstone formation also has silt and clay contents of 42 % and 21 %, respectively, with a cohesive strength of 37 kPa. While a SPB machine tunnelled in the highly weathered silty sandstone formation, mudcakes were formed in the cutterhead (Fig. 3). Initially, a dispersant was used on-site to disintegrate the mudcakes. However, due to the lack of instruments and methods to evaluate the disintegration effect of dispersants, the selected type of dispersant was found to be inappropriate, resulting in poor disintegration of the mudcakes. As the tunneling machine stopped close to a structure, prolonged downtime could potentially lead to collapse at the face, posing a threat to the safety of surface structures. In order to promptly eliminate the mudcakes, manual cleaning was eventually employed on-site. Some mudcakes were extracted for parameters analysis. The extracted mudcakes had a water content of 17 % ~ 22 % and a density of 2.10–2.13 g/cm³. The specific gravity of the mudcake was 2.85, resulting in calculated saturations ranging from 0.824 to 0.992.

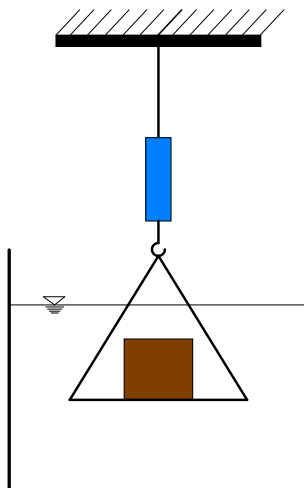


Fig. 2. Modified disintegration apparatus.

Table 1
Physical and mechanical parameters of each stratum.

Geotechnical name	Natural water content (%)	Quick shear		Content of silty and clay Particle (%)		Content of sand (%)		
		Cohesion force (kPa)	Internal friction angle (°)	0.005–0.075 mm	<0.005 mm	0.5–2 mm	0.25–0.5 mm	0.075–0.25 mm
Fully weathered argillaceous siltstone	19.6	30	21	42	23	10	11	14
Highly weathered argillaceous siltstone	17.0	36	24	42	21	10	13	13
Moderately weathered argillaceous siltstone	/	100	35	/	/	/	/	/

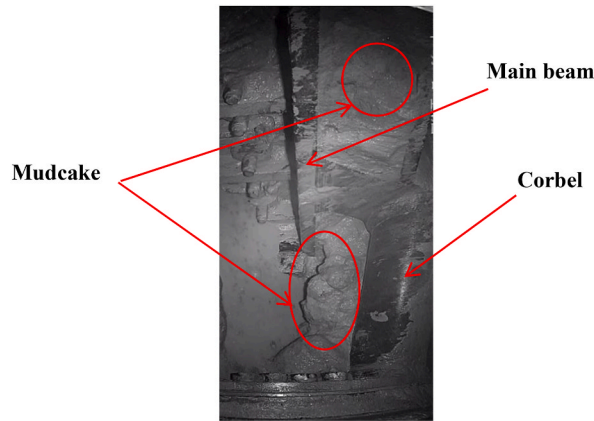


Fig. 3. Formation of mudcakes in cutterhead in the view from the back of the cutterhead to the front.

2.2. Testing materials

To assess the disintegration characteristics of mudcakes, the highly weathered silty sandstone excavated from foundation pits in the Guangzhou area was analyzed. The particle size distribution curve of the soil sample (Fig. 4) showed a maximum particle size of approximately 0.58 mm; among them, particles smaller than 0.075 mm accounted for about 90 % of the total particles. Based on the Chinese standard Code for the Design of Building Foundation [36], the soil sample was classified as silty clay. The specific gravity of the soil was 2.84. The powered soil and bentonite used for making slurry was tested by X-ray diffraction (XRD) apparatus for determining the mineral composition, as listed in Table 2. The main mineral compositions of the tested soil were quartz, albite and montmorillonite. The main mineral compositions of the bentonite were Na-montmorillonite, Ca-montmorillonite and soda feldspar. The chemical composition of the dispersant is listed in Table 3. The active ingredients of the dispersant were sodium lauryl alcohol polyoxyethylene ether sulfate and polyoxyethylene lauryl ether.

The comparison of parameters between the extracted mudcake and the compressed mudcake is shown in Table 4. Similar to the

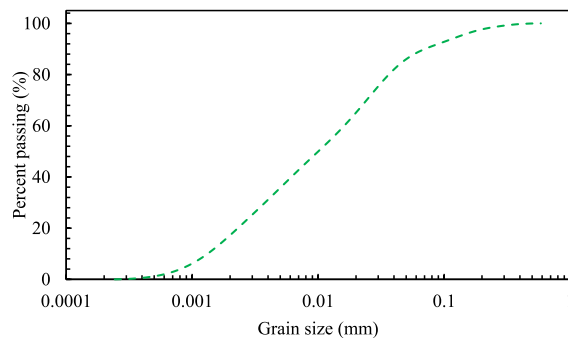


Fig. 4. Soil gradation curve.

Table 2
Mineral composition of the soil and bentonite.

Sample Name	Mineral composition	Mass percentage (%)
Highly weathered silty sandstone	Quartz	29.3
	Albite	24.9
	Montmorillonite	24.4
	Calcite	7.9
	Microcline feldspar	7.1
	Mica	6.4
Bentonite	Na-montmorillonite	48.8
	Ca-montmorillonite	14.1
	Soda feldspar	28.3
	Microcline	5.5
	Quartz	2.5
	Calcite	0.8

mudcake extracted from the shield machine, the compressed mudcake exhibited a water content of 20 % and a density of 2.12 g/cm³. Thus, the saturation compressed mudcake was 0.939.

2.3. Testing apparatus

The test apparatus includes a mudcake compression device and mudcake disintegration apparatus. The primary function of the mudcake compression device is to compact the mudcake, while the main purpose of the mudcake disintegration apparatus is to obtain the disintegration characteristics of the mudcake.

The schematic diagram and image of the mudcake compression device are shown in Fig. 5 (a) and Fig. 5 (b), respectively. The device comprised a piston, a specimen chamber, and a loading instrument. Soil samples were placed in the specimen chamber. The loading instrument applied pressure to the piston. As the piston moved downward, it compressed the soil sample till it came in contact with the edge of the specimen chamber. At this stage, increasing the pressure did not result in further downward movement of the piston, and the volume of the soil sample remained constant. As the volume of the specimen chamber remained constant, different compactness levels of mudcakes were obtained by controlling the water content and mass of the soil samples. The diameter of the mudcakes after pressing was 6 cm, with the height matching the diameter.

The schematic diagram and photograph of the mudcake disintegration apparatus are shown in Fig. 6 (a) and Fig. 6 (b), respectively. The apparatus consisted of a fixed support frame, a pressure sensor, a data acquisition instrument, a liquid container, and a hanging cage. The type of sensor is a resistive pressure sensor. The cage is made of stainless steel. The hanging cage contained the compressed mudcake, which was subsequently submerged in liquid. As the mudcake disintegrated, it fell into the container, thus increasing its mass. The pressure sensor and data acquisition instrument were used to measure and record the mass of the liquid container at various time intervals, which facilitated the determination of the mass variation of the disintegrated mudcake over time. This information was used to analyze the disintegration behavior of compressed mudcakes in various solutions. The diameter and height of the liquid container were 30 cm and 20 cm, respectively, while the diameter and height of the hanging cage were 10 cm and 15 cm, respectively.

2.4. Testing Procedure

The typical Marsh viscosity for slurry used in the slurry shield tunneling ranged from 34 s to 38 s. To examine the effect of bentonite slurry on the disintegration characteristics of mudcakes, the Marsh viscosity of the testing slurry was set to 30–40 s. The volume concentrations of the dispersant were 0 %, 2 %, 4 %, and 6 %. The testing conditions of all the mudcake disintegrating tests are summarized in Table 5. The test was conducted using the procedure described below:

- (1) The soil was dried in an oven at 105 °C for at least 24 h. Then, the dried soil clusters were broken up using a rubber hammer. A certain amount of dried soil was weighed and a specific quantity of water was sprayed onto it according to the testing requirements. After the soil sample was thoroughly mixed, it was placed in a container and sealed with cling film. The soil sample was incubated for at least 24 h to ensure sufficient water absorption (Fig. 7a).

Table 3
Chemical composition of the dispersant.

Chemical name	Mass percentage (%)
Sodium lauryl alcohol polyoxyethylene ether sulfate	4–5
Polyoxyethylene lauryl ether	0.5–0.7
Lauryl dimethylamine oxide	0.2–0.4
Sodium chloride	4–5
Water	89–91

Table 4
Comparison of mudcake parameters.

Soil type		Extracted mudcake	Compressed mudcake
Specific gravity		2.85	2.84
Atterberg limits (%)	Liquid limit	30.7	29.8
	Plastic limit	20.1	19.7
Water content (%)		17~22	20
Density (g/cm ³)		2.10–2.13	2.12
Saturation		0.824–0.992	0.939

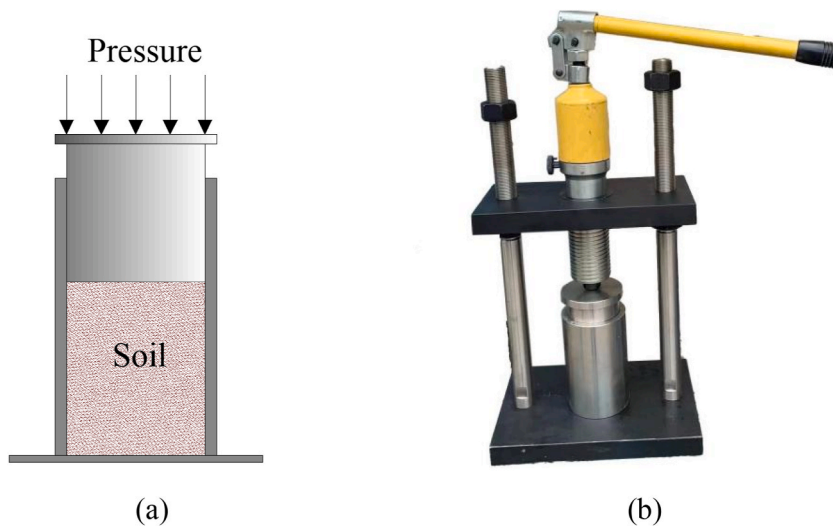


Fig. 5. Mudcake compression device: (a) a schematic diagram, and (b) a photograph of the device.

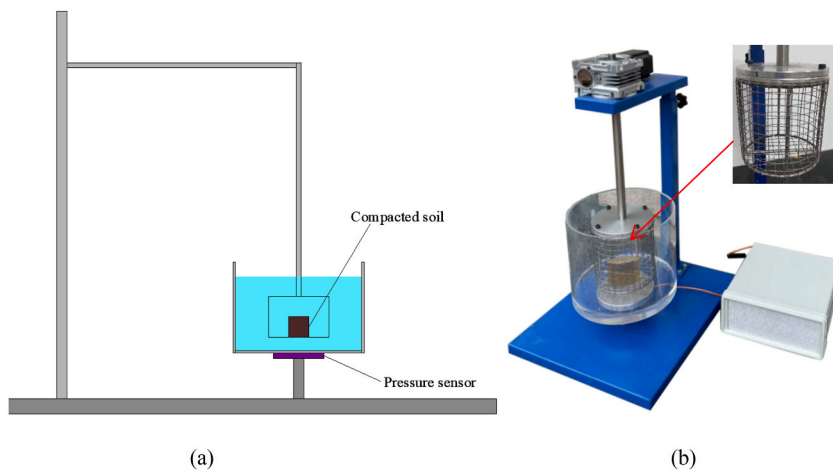


Fig. 6. Mudcake disintegration apparatus: (a) A schematic diagram and (b) a photograph of the apparatus.

- (2) Weighed 359.5g of the moistened soil and divided it into three equal portions. After putting the first portion into the specimen chamber, the piston was inserted into the chamber. The soil sample was compressed using a loading instrument, while the compression height was controlled. Then, the surface of the sample was scraped. The second portion of the soil sample was added, and the previous step was repeated. After the final layer has been constructed, the test specimen should be loaded and compressed until the height reaches 6 cm. At this time, the soil sample was fully compressed (Fig. 7b).
- (3) After the soil sample was compressed, the mudcake pressing device was removed, and the piston of the device was taken out. The specimen chamber was placed upside down on the demolding base. The demolder was aligned with the cavity of the

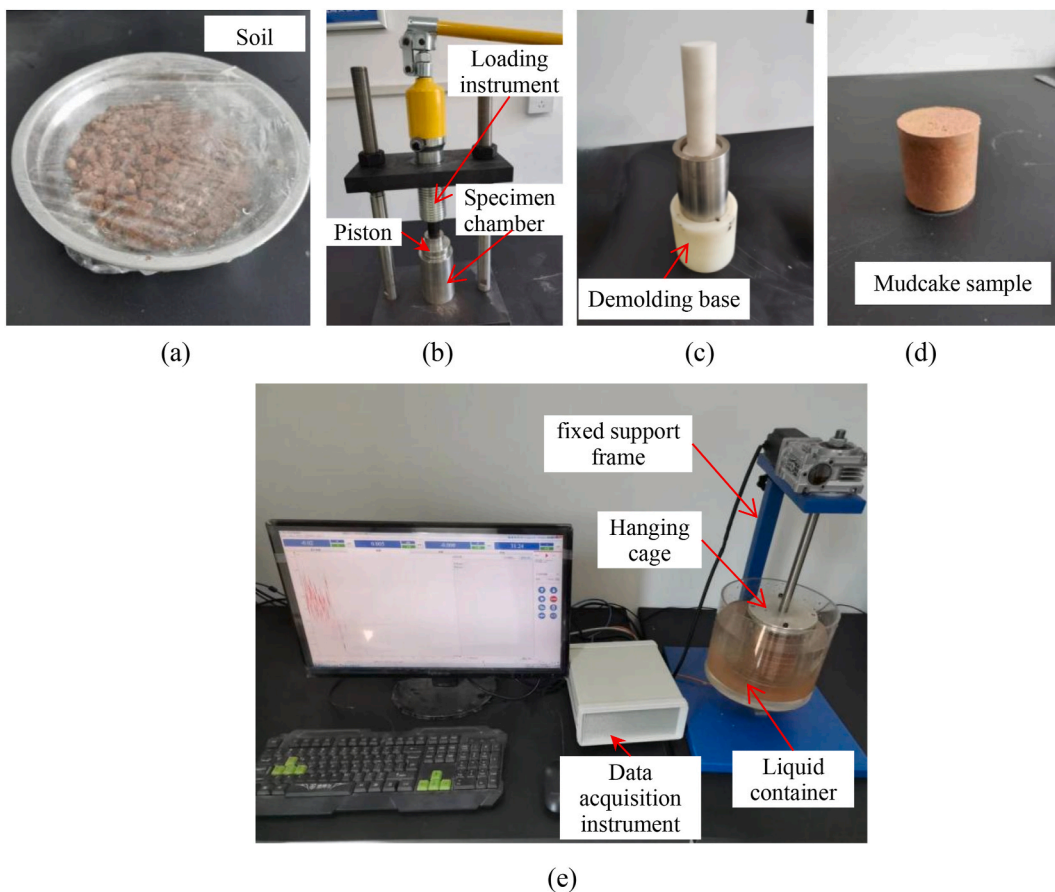


Fig. 7. Testing Procedure: (a) soil sample wetting, (b) soil sample compression, (c) soil sample demolding, (d) mudcake, and (e) mudcake disintegration.

Table 5
Overview of the testing conditions.

Liquid	Parameter type	Data
Water	–	–
Dispersant solution	volume concentration (%)	0, 2, 4, 6
Slurry	Marsh viscosity (s)	30, 35, 40

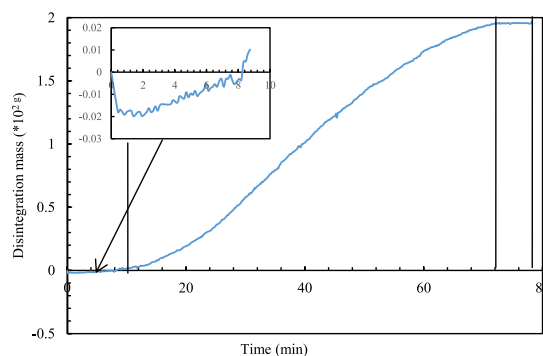


Fig. 8. Disintegration curve of the mudcake in water.

specimen chamber (Fig. 7c). Then, the plastic piston was used to apply a force to push out the soil sample, and a mudcake sample was obtained with a specific degree of compression (Fig. 7d).

- (4) Approximately three-fourths of the liquid container was filled with water and placed on the support base. The height of the fixed support frame was adjusted to its highest point and secured. The mudcake was placed in the hanging cage. The height of the fixed support frame was gradually decreased until the mudcake was completely submerged in the liquid.
- (5) The reading on the pressure sensor was changed to zero and the timer was started (Fig. 7e). The pressure sensor data were acquired and recorded at a frequency of 10 s per reading.
- (6) When mudcake disintegration was complete or the pressure sensor readings no longer changed, the recording was stopped. The data were stored, and a graph of the pressure sensor readings over time was plotted.

3. Testing results

3.1. Mudcake disintegration curve in water

The variation in the disintegration mass of the mudcake in water with time is shown in Fig. 8. The disintegration of the mudcake could be categorized into three stages, including the initial stage, the rapid disintegration stage, and the stable stage. The initial stage required approximately 8 min after starting the test. The water in the liquid container was relatively clear during the initial stage (Fig. 9a), which suggested that the mudcake underwent minimal disintegration. The disintegration mass of the mudcake had a negative value, indicating an increase in the mudcake mass. This primarily occurred due to the absorption of water by the mudcake at the initial stage when it was immersed. The mass of absorbed water exceeded the mass of the disintegrated mud cake. This led to an overall increase in the mudcake mass. As the rate of water absorption by the mudcake decreased, the rate of mudcake disintegration increased, resulting in a shift toward a positive value in the mass of mudcake disintegration. The rapid disintegration stage started around 12 min after initiating the test. The mudcake underwent rapid disintegration, accompanied by an increase in the mass of mudcake disintegration in the rapid disintegration stage. The water in the liquid container became cloudy (Fig. 9b). The stable stage was reached around 70 min after starting the test. The mass of mudcake disintegration showed a negligible increase during the stable stage, indicating the complete disintegration of the mudcake (Fig. 9c).

3.2. Effect of dispersant on mudcake disintegration

The disintegration curve of the mudcake under the effect of a dispersant is shown in Fig. 10. The trend of the mudcake disintegration curve in the dispersant solution was similar to that observed for mudcake disintegration in water. The disintegration process of the mudcake could be categorized into three stages: the initial stage, the rapid disintegration stage, and the stable stage. When the pressure sensor reading remained constant for 10 min, it was considered that the mudcake had completely disintegrated. For dispersant solution concentrations of 0 %, 2 %, 4 %, and 6 %, the complete disintegration of the mudcake required 78.19 min, 75.42 min, 65.83 min, and 50.14 min respectively. Using a 6 % dispersant solution increased the mudcake disintegration efficiency by 35.87 % compared to the disintegration efficiency recorded in water. Therefore, immersing the mudcake in a dispersant solution significantly increased the disintegration rate. Adding the dispersant eliminated negative disintegration mass values, i.e., the mass of the mudcake was stable during the initial stage. This phenomenon was primarily attributed to the capacity of the dispersant to accelerate the disintegration rate. Initially immersing the mudcake in the dispersant solution caused the disintegration rate to exceed the water absorption rate, which prevented an increase in the mudcake mass.

3.3. Effect of bentonite slurry on mudcake disintegration

The disintegration curve of the mudcake in bentonite slurry is shown in Fig. 11. Unlike in water and dispersant solution, in bentonite slurry, as the time increased, the disintegration mass of the mudcake initially decreased and then stabilized. The disintegration mass of the mudcake was negative, which indicated an increase in mudcake mass. Thus, the presence of bentonite effectively inhibited mudcake disintegration. The disintegration of the mudcake in the bentonite slurry included an initial stage and a stable stage. In the initial stage, the mudcake absorbed water from the slurry, resulting in a slow increase in mass. In the stable stage, the mudcake surface became saturated and encapsulated by bentonite (Fig. 12), preventing further water absorption and resulting in minimal changes in mass. As Marsh viscosity increased from 30 s to 40 s, the quantity of water absorbed by the mudcake decreased, resulting in a smaller increase in mass.

4. Discussion

The dispersion-assisted mudcake disintegration is a commonly used on-site removal method for mudcakes. However, there is a lack of devices and methods to evaluate the effectiveness of dispersion. The mudcake compression device and mudcake disintegration device proposed in this study can effectively evaluate the performance of different dispersion agents, reducing costs for mudcake removal in construction sites [37,38]. However, this device also has certain limitations. As shown in Fig. 8, although the initial weight of the mudcake samples was the same, the disintegration mass after complete disintegration varies. This is mainly because during the mudcake disintegration process, a portion of the soil does not fall into the liquid container but adheres to the cage, resulting in different mudcake disintegration masses after the test.

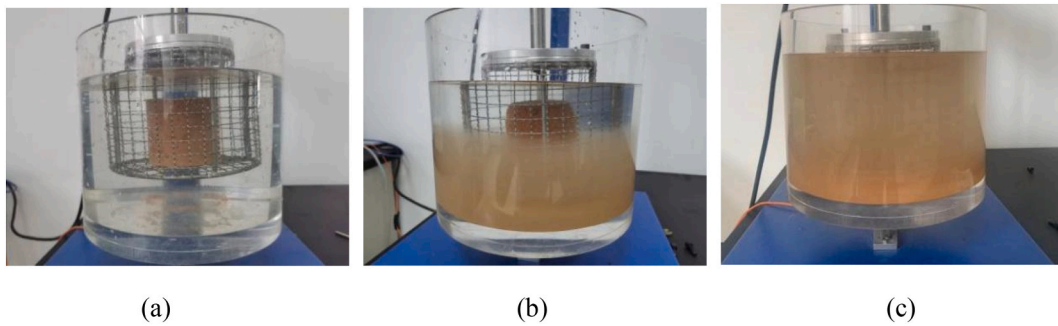


Fig. 9. Images of different mudcake disintegration stages in water: (a) the initial stage, (b) the rapid disintegration stage, and (c) the stable stage.

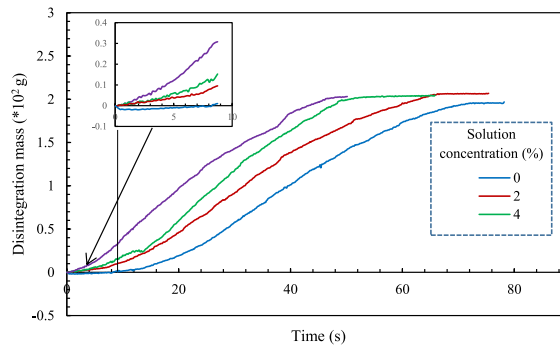


Fig. 10. Disintegration curves of the mudcake in dispersant solutions.

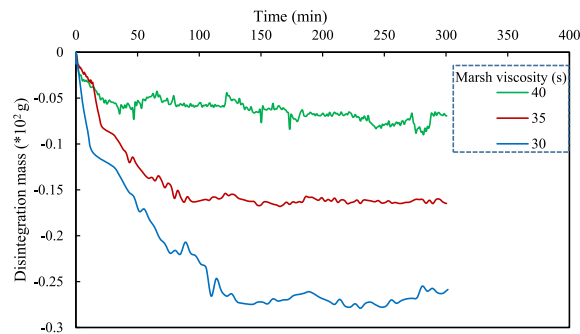


Fig. 11. Disintegration curves of the mudcake in bentonite slurry.

The Marsh viscosity of pure water is 26s. By adding a small amount of bentonite to pure water, a slurry with a Marsh viscosity of 30s can be prepared. By comparing Figs. 6 and 9, it can be observed that the mudcake can disintegrate in pure water. However, after adding a small amount of bentonite, the mudcake can no longer disintegrate. This indicates that a small amount of bentonite can inhibit the disintegration of the mudcake. In the process of slurry shield tunneling, it is necessary to maintain a balanced tunnel face using bentonite and remove the excavated soil. After the mudcakes form on the cutterhead and cutting tools, the operators often inject low-viscosity slurry into the chamber and increase the mud circulation rate, attempting to disintegrate the mudcake through this method. However, the testing results of this study show that even in a mud with a Marsh viscosity of 30s, the mudcake cannot disintegrate. Therefore, the method of using circulated low-viscosity slurry to disintegrate the mudcake is not feasible. Not only does the mudcake not disintegrate, but in severe cases, excessive removal of excavated soil due to slurry circulation can lead to collapse of the shield face, posing a serious threat to construction safety.

5. Conclusions

When a TBM tunnels in cohesive strata, mudcakes are prone to form. The chamber of a slurry shield machine is filled with slurry,



Fig. 12. Mudcake encapsulated by bentonite.

where mudcakes are immersed. Following mudcake formation, dispersants are employed for disintegration. Thus, this study investigates the impact of slurry and dispersant on the disintegration characteristics of mudcakes. The primary conclusions were as follows:

- (1) A mudcake compression device and a mudcake disintegration apparatus were developed. The primary innovation of the mudcake compression device is the ability to achieve set compaction levels of mudcakes by controlling the water content and mass of the soil samples. The key innovation of the mudcake disintegration apparatus is its capability to analyze the disintegration behavior of compressed mud cakes in different solutions.
- (2) The disintegration of the mudcake could be categorized into three stages: the initial stage, the rapid disintegration stage, and the stable stage. In the initial stage, the mudcake absorbed water, resulting in a negative initial disintegration mass, which increased gradually but with minimal overall change. The rapid disintegration stage led to a rapid increase in the mass of disintegration. In the stable stage, the disintegration mass of the mudcake remained constant, indicating complete disintegration.
- (3) Immersing the mudcakes in dispersant solutions with a concentration of 2 %, 4 % or 6 % significantly increased the disintegration rate. The disintegration rate increased with an increase in the dispersant concentration. The addition of dispersant prevented the disintegration mass from becoming negative during the initial stage of disintegration.
- (4) The disintegration of the mudcake in bentonite slurry could be categorized into two stages: the initial stage and the stable stage. The disintegration mass initially decreased and then stabilized with an increase in disintegration time. The disintegration mass of the mudcake became negative, indicating an increase in mudcake mass. These changes showed that even a bentonite slurry with a Marsh viscosity of 30 s significantly inhibited mud cake disintegration.

In this study, we introduced a self-manufactured mudcake compression device and mudcake disintegration apparatus. The effects of dispersants and bentonite slurry on the disintegration characteristics of mudcakes were investigated. However, many factors that affect the disintegration characteristics of mudcakes, such as the size, compaction, and saturation of mudcakes, need to be further investigated.

Data availability statement

Data will be made available on request.

CRediT authorship contribution statement

Pengfei Liu: Writing – review & editing, Writing – original draft, Funding acquisition, Conceptualization. **Zhao Yang:** Writing – review & editing, Investigation, Formal analysis, Data curation. **Fuquan Ji:** Resources, Methodology, Investigation. **Peishuai Chen:** Supervision, Software, Project administration, Methodology. **Qinxin Hu:** Writing – review & editing, Validation, Supervision, Software. **Xiong He:** Visualization, Validation, Supervision, Resources.

Declaration of competing interest

The authors declare that they have no known competing financial interests or personal relationships that could have appeared to influence the work reported in this paper.

Acknowledgements

The financial supports from the China Postdoctoral Science Foundation (Grant No. 2022M723536) and open fund project of Key Laboratory of Safe Construction and Intelligent Maintenance for Urban Shield Tunnels of Zhejiang Province (Grant No. HZCU-UST-23-03) are acknowledged and appreciated. The authors are also grateful to the help from Shihong Zhai, Xiaofeng Tan, Guanjun You, Haijiang Xu, Gang Li, Qing Yang, Heng Sun, Chao Xu, Zhiyong Yang and Jun Yu in CCCC Second Harbor Engineering Company Ltd.

References

- [1] Salmanpour, Farjam, et al, Effect of soil conditioning on the permeability of coarse-grained soil in mechanized tunnelling, *Heliyon*. 9 (12) e22640.
- [2] H. Pavolová, T. Bakalár, K. Kyšľa, Miroslav Klimek, Z. Hajduová, M. Zawada, The analysis of investment into industries based on portfolio managers, *Acta Montan. Slovaca* 26 (1) (2021) 161–170.
- [3] S. Wang, P. Liu, Z. Gong, P. Yang, Auxiliary air pressure balance mode for EPB shield tunneling in water-rich gravelly sand strata: feasibility and soil conditioning, *Case Stud. Constr. Mater.* 6 (2022) e00799.
- [4] P. Liu, S. Wang, L. Ge, M. Thewes, J. Yang, Y. Xia, Changes of Atterberg limits and electrochemical behaviors of clays with dispersants as conditioning agents for EPB shield tunnelling, *Tunn. Undergr. Space Technol.* 73 (2018) 244–251.
- [5] M. Thewes, F. Hollmann, Assessment of clay soils and clay-rich rock for clogging of TBMs, *Tunn. Undergr. Space Technol.* 57 (2016) 122–128.
- [6] U. Burbaum, I. Sass, Physics of adhesion of soils to solid surfaces, *Bull. Eng. Geol. Environ.* 76 (3) (2017) 1097–1105.
- [7] M. Feinendegen, M. Ziegler, G. Spagnoli, A new laboratory test to evaluate the problem of clogging in mechanical tunnel driving with EPB-shields, *Rock Mechanics in Civil and Environmental Engineering* (2010) 449–452.
- [8] J. Zhai, Q. Wang, D. Yuan, W. Zhang, H. Wang, X. Xie, I. Shahrour, Clogging risk early warning for slurry shield tunneling in mixed mudstone–gravel ground: a Real-Time Self-Updating Machine Learning Approach, *Sustainability* 14 (2022) 1368.
- [9] X. Li, Y. Yang, X. Li, H. Liu, Criteria for cutting lead clogging occurrence during slurry shield tunneling, *Appl. Sci.* 12 (2022) 1001.
- [10] Z. Chen, A. Bezuijnen, Y. Fang, K. Wang, R. Deng, Experimental study and field validation on soil clogging of EPB shields in completely decomposed granite, *Tunn. Undergr. Space Technol.* 120 (2022) 104300.
- [11] B. Zhuo, Y. Fang, M. Zhu, Y. Wang, Y. Yao, G. Xu, Combined conditioning of dispersant and foam agent for the soil with different clay minerals: an experimental study, *Bull. Eng. Geol. Environ.* 82 (2023) 248.
- [12] A. Khabbazi, M. Ghafoori, A. Cheshomi, Experimental and laboratory assessment of clogging potential based on adhesion, *Bull. Eng. Geol. Environ.* 78 (1) (2019) 605–616.
- [13] R. Zumsteg, M. Ploetze, A. Puzrin, Reduction of the clogging potential of clays: new chemical applications and novel quantification approaches, *Geotechnique* 63 (4) (2013) 276–286.
- [14] L. Langmaack, K.F. Lee, Difficult ground conditions? Use the right chemicals! Chances–limits–requirements, *Tunn. Undergr. Space Technol.* 57 (2016) 112–121.
- [15] D. Peila, D. Martinelli, C. Todaro, A. Luciani, Soil conditioning in EPB shield tunnelling—An overview of laboratory tests, *Geomechanics and Tunnelling* 12 (5) (2019) 491–498.
- [16] S. Wang, Z. Zhou, P. Liu, Z. Yang, Q. Pan, W. Chen, On the critical particle size of soil with clogging potential in shield tunneling, *J. Rock Mech. Geotech. Eng.* 15 (2023) 477–485.
- [17] B. Maidl, M. Herrenknecht, U. Maidl, G. Wehrmeyer, *Mechanised Shield Tunnelling*, second ed., Ernst and Sohn, Berlin, 2012.
- [18] R. Zumsteg, A. Puzrin, Stickiness and adhesion of conditioned clay pastes, *Tunn. Undergr. Space Technol.* 31 (2012) 86–96.
- [19] R. Zumsteg, M. Plötze, A.M. Puzrin, Effect of soil conditioners on the pressure and rate-dependent shear strength of different clays, *J. Geotech. Geoenviron. Eng.* 138 (9) (2012) 1138–1146.
- [20] D. Oliveira, M. Thewes, M.S. Diederichs, L. Langmaack, EPB tunnelling through clay-sand mixed soils: proposed methodology for clogging evaluation, *Geomechanics and Tunnelling* 11 (4) (2018) 375–387.
- [21] D. Oliveira, EPB Excavation and Conditioning of Cohesive Mixed Soils: Clogging and Flow Evaluation, Kingston Queen’s University, 2018.
- [22] F.S. Hollmann, M. Thewes, Assessment method for clay clogging and disintegration of fines in mechanised tunnelling, *Tunnelling Undergr. Space Technol.* 37 (2013) 96–106.
- [23] P. Liu, S. Wang, Y. Shi, J. Yang, J. Fu, F. Yang, Tangential adhesion strength between clay and steel for various soil softnesses, *J. Mater. Civ. Eng.* 31 (2019) 04019048.
- [24] S. Wang, P. Liu, Q. Hu, J. Zhong, Effect of dispersant on the tangential adhesion strength between clay and metal for EPB shield tunnelling, *Tunn. Undergr. Space Technol.* 95 (2020) 103–144.
- [25] X. Xiao, Y. Xia, X. Mao, Y. Wang, Z. Fang, F. Wang, H. Zhao, Effect of the nozzle structure of the large-diameter slurry shield cutterhead on the scouring characteristics, *J. Braz. Soc. Mech. Sci. Eng.* 42 (4) (2020) 157.
- [26] P. Liu, S. Sun, Z. Yang, F. Ji, Impact of anti-sticking coating technology on shear strength at the clay-metal interface in cohesive strata, *Front. Earth Sci.* 11 (2023) 1216614.
- [27] Y. Fang, Y. Yao, T. Song, L. Wei, P. Liu, B. Zhuo, Study on disintegrating characteristics and mechanism of cutterhead mud-caking in cohesive strata, *Bull. Eng. Geol. Environ.* 81 (2022) 510.
- [28] Kristina Razminien, Irina Vinogradova, Manuela Tvaronavi, ien, Clusters in transition to circular economy: evaluation of relation, *Acta Montan. Slovaca* 26 (3) (2021) 455–465.
- [29] Josef Maroušek, Lukáš Trakal, Techno-economic analysis reveals the untapped potential of wood biochar, *Chemosphere* 291 (1) (2022) 133000.
- [30] Y. Bissonnais, Aggregate stability and assessment of soil crustability and erodibility: I. Theory and methodology, *Eur. J. Soil Sci.* 47 (4) (1996) 425–437.
- [31] W.W. Emerson, D.J. Greenland, *Soil Aggregates—Formation and Stability*, Springer, Boston, MA, 1990, pp. 485–511.
- [32] I. Shainberg, J. Lety, Response of soils to sodic and saline conditions, *Hilgardia* 52 (2) (1984) 1–57.
- [33] J.P. Quirk, The significance of the threshold and turbidity concentrations in relation to sodicity and microstructure, *Soil Res.* 39 (6) (2001) 1185–1217.
- [34] H. Mao, Y. Yang, H. Zhang, et al., A critical review of the possible effects of physical and chemical properties of subcritical water on the performance of water-based drilling fluids designed for ultra-high temperature and ultra-high pressure drilling applications, *J. Journal of Petroleum Science and Engineering* 187 (2020) 106795.
- [35] Z. Yang, P. Liu, P. Chen, S. Li, F. Ji, Clogging prevention of slurry–earth pressure balance dual-mode shield in composed strata with medium–coarse sand and argillaceous siltstone, *Appl. Sci.* 13 (2023) 2023.
- [36] GB 50007–2019, Chinese Standard Code for the Design of Building Foundation, China Architecture and Building Press, 2019 (in Chinese).
- [37] Marek Vochozka, Jakub Horák, Tomáš Krulický, Pedro Pardal, Predicting future brent oil price on global markets, *Acta Montan. Slovaca* 25 (3) (2020) 375–392.
- [38] M. Vochozka, Z. Rowland, P. Šulěr, J. Maroušek, The influence of the international price of oil on the value of the EUR/USD exchange rate, *J. Cryptol.* 12 (2020) 167–190.